Benzyl isothiocyanate suppresses development and metastasis of murine mammary carcinoma by regulating the Wnt/β-catenin pathway

BEI XIE[1], LEI ZHAO[2], LANLAN GUO[3], HANG LIU[3], SIYU FU[3], WENJUAN FAN[3], LI LIN[1], JING CHEN[1], BEI WANG[1], LINLAN FAN[1] and HULAI WEI[1]

[1]Key Laboratory of Preclinical Study for New Drugs of Gansu Province, School of Basic Medical Sciences, Lanzhou University, Lanzhou, Gansu 730000; [2]Shaanxi Meili Omni-Honesty Animal Health Co., Ltd., Xi'an, Shaanxi 710000; [3]Students of Clinical Medicine, School of Medicine, Lanzhou University, Lanzhou, Gansu 730000, P.R. China

Received October 11, 2018; Accepted May 23, 2019

DOI: 10.3892/mmr.2019.10390

Abstract. Benzyl isothiocyanate (BITC) has been reported to exhibit antitumor properties in various cancer types; however, the underlying mechanisms of its action remain unclear. In the present study, the efficacy of BITC on murine mammary carcinoma cells was evaluated *in vitro* and *in vivo*, revealing a potential mechanism for its action. *In vivo* bioluminescence imaging indicated dynamic inhibition of murine mammary carcinoma cell growth and metastasis by BITC. A terminal deoxynucleotidyl transferase-mediated dUTP nick end labeling assay demonstrated that BITC also induced apoptosis. BITC further exhibited antitumorigenic activity in 4T1-Luc cells *in vitro* via the inhibition of cell proliferation, induction of apoptosis and cell cycle arrest, and inhibition of cell migration and invasion. Furthermore, the activity of key molecules of the adenomatous polyposis coli (APC)/β-catenin complex was altered following treatment with BITC, which suggested a potential role for the APC/β-catenin complex in the BITC-mediated induction of apoptosis and inhibition of metastasis in murine mammary carcinoma. BITC upregulated the activity of glycogen synthase kinase-3β and APC proteins, whereas it downregulated β-catenin expression. The inhibition of metastasis was accompanied with the downregulation of vimentin and upregulation of E-cadherin. Conversely, BITC did not exhibit toxicity or side effects in the normal mammary epithelial cell line MCF-10A. The present study indicated that BITC exhibited anticancer properties due to the induction of breast cancer cell apoptosis and inhibition of breast cancer cell metastasis mediated by the Wnt/β-catenin signaling pathway.

Correspondence to: Dr Hulai Wei, Key Laboratory of Preclinical Study for New Drugs of Gansu Province, School of Basic Medical Sciences, Lanzhou University, 199 Donggang West Road, Lanzhou, Gansu 730000, P.R. China
E-mail: weihulai@lzu.edu.cn

Key words: apoptosis, benzyl isothiocyanate, metastasis, murine mammary carcinoma, Wnt/β-catenin pathway

Introduction

Breast cancer is the most frequently diagnosed cancer and is considered to be the second leading cause of cancer-associated mortality in women (1,2). Breast cancer is routinely treated with surgery, hormone therapy, chemotherapy, radiation therapy or a selective combination; however, these current therapies are not completely effective, and have also been reported to induce unwanted side effects and toxicities (2).

Epidemiologic studies have demonstrated that specific agents in dietary plants may serve tumor-suppressive and therapeutic roles (3). Pertinent to this, statistical studies have reported that dietary intake of cruciferous vegetables may reduce the risk of cancer incidence and progression (4). Isothiocyanates (ITCs) are mainly derived from cruciferous vegetables, and may be potentially used for the prevention of various types of cancer, including lung, liver, breast and colon cancers (5,6). Benzyl isothiocyanate (BITC) is a phytochemical that has demonstrated preventive efficacy in cancer xenograft and transgenic mouse models in the absence of notable side effects or toxicity (7-10). Administration of BITC markedly suppressed the incidence and stage of mammary hyperplasia and the progression of carcinoma in mice (7,9,10). *In vitro* studies have reported that BITC acts via diverse mechanisms to induce antitumorigenic effects, including the inhibition of cell proliferation and induction of apoptosis, modulation of cell cycle arrest and inhibition of cancer cell migration and invasion (11-13). Additional studies revealed that BITC regulated various signaling pathways; for example, BITC induced apoptosis by inhibiting the phosphatidylinositide 3-kinase (PI3K) pathway, or by activating the p53-liver kinase B1 (LKB1) and/or the p73-LKB1 pathways (11,12). Additionally, BITC induced reactive oxygen species (ROS)-dependent suppression of STAT3 protein expression, and inhibited migration and invasion by affecting the MAPK signaling pathway and the activity of matrix metalloproteinase-2/-9 enzymes (13-16). Numerous studies investigated the effects of BITC on cancer

prevention and treatment; however, the underlying mechanisms of its antitumor properties remain unclear.

Dysregulation of the Wnt signaling pathway is a hallmark of several aggressive human cancers (17). At present, the Wnt signaling pathway is considered an attractive area of research with regard to cancer treatment and therapy (18). The key signaling molecule of this pathway is β-catenin, whose activity is mainly regulated by a destruction complex consisting of adenomatous polyposis coli (APC), Axin2 and glycogen synthase kinase-3β (GSK-3β) (19). Wnt/β-catenin serves various roles in numerous types of cancer cell in response to different treatments, including the regulation of cell proliferation, migration, apoptosis and epithelial-to-mesenchymal transition (EMT) (20-22).

BITC inhibited human breast cancer cell tumorigenesis via the suppression of the forkhead box H1 (FOXH1)-mediated Wnt/β-catenin pathway (22); however, whether BITC acts via the Wnt signaling pathway in murine mammary carcinoma cells is unclear. In the present study, the ability of BITC to inhibit the growth and migration of murine breast cancer cells was investigated, as were the associated mechanisms underlying this process.

Materials and methods

Reagents, cells and animals. BITC was purchased from Sigma-Aldrich (Merck KGaA). SYBR Premix Ex Taq™ and PrimeScript™ RT kits were obtained from Takara Bio, Inc. Antibodies specific for APC (cat. no. sc-896; Santa Cruz Biotechnology, Inc.), β-catenin (cat. no. sc-7963; Santa Cruz Biotechnology, Inc.), phosphorylated (p)-β-catenin (cat. no. GTX50256; GeneTex, Inc.), Wnt2 (cat. no. ab109222; Abcam), E-cadherin (cat. no. 3195; Cell Signaling Technology, Inc.), vimentin (cat. no. GTX100619; GeneTex, Inc.), Axin2 (cat. no. ab109307; Abcam), GSK-3β (cat. no. ab32391; Abcam), cyclin D1 (cat. no. ab134175; Abcam), c-Myc (cat. no. ab32072; Abcam) and β-actin (cat. no. TA-09; Zhongshan Jinqiao Bio-Technology Co., Ltd.) were used in the present study. BITC was dissolved in dimethyl sulfoxide.

The murine mammary carcinoma cell line 4T1-Luc (stable transfection of the firefly luciferase gene) was purchased from the Cold Spring Harbor Laboratory and cultured in DMEM (HyClone; GE Healthcare Life Sciences) supplemented with 10% fetal bovine serum (Biological Industries) in the presence of 1% antibiotics (100 U/ml penicillin and 100 μg/ml streptomycin) and 2 mM L-glutamine at 37˚C in a 5% CO_2 humidified atmosphere. The normal mammary epithelial cell line MCF-10A was obtained from the American Type Culture Collection and was cultured in DMEM/F-12 medium (Thermo Fisher Scientific, Inc.) supplemented with 5% horse serum (Thermo Fisher Scientific, Inc.), 20 ng/ml epidermal growth factor (PeproTech, Inc.), 100 ng/ml cholera toxin (Sigma-Aldrich; Merck KGaA), 10 μg/ml human insulin, 100 U/ml penicillin and 100 μg/ml streptomycin. The cells were maintained at 37˚C and 5% CO_2 in a humidified incubator.

Female BALB/c mice (specific pathogen-free grade, 8 weeks old, n=72 mice, 20-24 g) were provided by the Laboratory Animal Center of Lanzhou University. The mice were housed in the barrier system facilities of the Key Laboratory of Preclinical Studies for New Drugs of Gansu Province (School of Basic Medical Sciences, Lanzhou University), which specializes in preclinical studies for novel drugs. Food and water was provided *ad libitum* in the facility, and the animals were maintained in a specific pathogen-free condition at 20-26˚C, 40-70% humidity with a 12-h light/dark cycle. All the animal procedures were ethically approved by the Laboratory Animal Science and Technology Management Committee of the Lanzhou University School of Basic Medical Sciences, and were conducted in accordance with the Guide for Care and Use of Laboratory Animals (23).

Cell viability assay. A cell viability assay was performed as previously described (24). Briefly, cells were plated in 96-well plates at an initial density of $4x10^3$ cells/well and cultured overnight. Subsequently, the medium was replaced with fresh complete medium containing various concentrations of BITC (0, 1, 2.5, 5, 10, 20 and 40 μM). The cells were incubated for 24, 48 and 72 h. A total of 10 μl MTT solution was then added to each well, followed by incubation for 4 h at 37˚C. 10% SDS was added to each of the wells, and incubated overnight at 37˚C to dissolve the formazan crystals. Finally, the absorbance values of each well were measured at 570 nm, and the readings were quantified using a Powerwave X plate reader (Bio-Tek Instruments, Inc.). Cell proliferation inhibitory rates were calculated.

Clonogenicity assay. 4T1-Luc cells were pretreated with various concentrations of BITC (0, 1, 2.5, 5, 10 and 20 μM) for 24 h. Subsequently, the cells were digested with 0.25% trypsin at 37˚C for 2-3 min, and single cell suspensions were seeded in 6-well plates at a density of 1,000 cells/well. Following 2 weeks of culture at 37˚C in a 5% CO_2 humidified atmosphere, the cells in each well were washed with 1 ml phosphate buffered saline (PBS) and fixed with 0.5 ml 100% methanol at room temperature for 30 min. Subsequently, the cells were stained with crystal violet (0.1% in 20% methanol) at room temperature for 30 min. Excess crystal violet was removed using dH_2O. The colony numbers were assessed visually using Olympus IX81 inverted microscope (Olympus Corporation) at x40 magnification, and only colonies containing >50 cells with normal morphology were counted.

Morphological characteristics. The cells were seeded into 6-well plates at a density of $1x10^5$ cells/well in 2 ml of medium. Subsequently, they were treated with BITC as aforementioned and observed under an inverted microscope (IX81; Olympus Corporation) or mounted onto slides. The cells on the slides were stained using Wright-Giemsa at room temperature for 15 min and observed under a light microscope (AX80; Olympus Corporation).

Cells were sequentially fixed with 2% glutaraldehyde at 4˚C for 48 h and 1% OsO_4 at 4˚C for 90 min for ultrastructural observation. Following dehydration, thin sections (50-70 nm) embedded by resin were stained with uranyl acetate for 30 min and lead citrate for 15 min at room temperature for visual investigation under a JEM 1230 transmission electron microscope (JEOL, Ltd.). Images were acquired digitally from a randomly selected pool of 10-15 fields for each condition at x5,000 magnification.

Apoptotic and cell cycle analyses. The induction of apoptosis by BITC was determined using an Annexin V/dead cell apoptosis kit (cat. no. V13241; Invitrogen; Thermo Fisher Scientific, Inc.). Samples were gently suspended in 100 μl binding buffer containing 5 μl of Annexin V-FITC and 5 μl propidium iodide (PI), and further incubated for 15 min in the dark at room temperature. Finally, cells were suspended in 500 μl binding buffer and were detected by flow cytometry (Epics XL; Beckman Coulter, Inc.) and analyzed with Expo 32 software (Beckman Coulter, Inc.). The apoptotic rate was determined for each condition as follows: Apoptotic rate=(apoptotic rate $_{\text{early apoptosis}}$ + apoptotic rate $_{\text{late apoptosis}}$) x100%.

Cells were treated with various concentrations of BITC (0, 2.5, 5 and 10 μM) for 24 and 48 h, and then washed with ice-cold PBS and fixed in cold 70% ethanol overnight. Prior to analysis, cells were washed with PBS and incubated with PI for 30 min at room temperature in the dark. The DNA contents were analyzed with Multicycle for Windows using an Epics XL flow cytometer (Beckman Coulter, Inc.).

Mitochondrial transmembrane potential (MTP) detection. Cells were washed with PBS and incubated with 1 μM rhodamine 123 (Rh123) in the dark for 30 min at 37˚C. The mean fluorescence intensity (MFI) of Rh123-labeled cells was analyzed with System II software version 3.0 (Epics XL; Beckman Coulter, Inc.) using a flow cytometer (Epics XL; Beckman Coulter, Inc.) at an excitation and emission wavelength of 488 and 525 nm, respectively. A minimum of $1x10^4$ events/sample were acquired.

Wound healing assay. For the wound healing assay, cells were seeded in 6-well plates and grown in complete medium to ~100% confluence. Subsequently, they were washed with serum-free medium and serum-starved for 16 h. A 1-mm wide scratch was made across the cell layer using a sterile pipette tip. The plates were photographed immediately following scratching. Following treatment of the cells with various concentrations of BITC (0, 1, 2.5, 5, 10 and 20 μM) for 0, 10 and 24 h, the plates were photographed at identical locations to the initial images using Olympus IX81 inverted microscope (Olympus Corporation) at x100 magnification.

Cell invasion and migration assays. The ability of cells to penetrate a synthetic basement membrane was assessed using a Matrigel-Boyden chamber invasion assay (BD Biosciences). Transwell inserts (6.5 mm) fitted with polycarbonate filters (8-μm pore size) were used. The upper chambers of the wells were coated with Matrigel (BD Biosciences). A total of $1x10^5$ 4T1-Luc cells were cultured in serum-free medium containing treatments as aforementioned. The cells were allowed to penetrate at 37˚C for 24 h. The lower chambers of the plate were filled with complete medium. Following 24 h of incubation, the cells remaining in the upper part of the insert membrane were removed by gentle scraping with a sterile cotton swab. The cells that had invaded through the Matrigel to the bottom of the insert were fixed in 4% paraformaldehyde at room temperature for 30 min and stained with crystal violet (0.1% in 20% methanol) at room temperature for 30 min. Five random fields were imaged (magnification, x100) using Olympus IX71 inverted microscope (Olympus Corporation). All presented data were obtained from at least three independent experiments performed in duplicate. The migration assay was performed in the same manner as the invasion assay in the absence of Matrigel.

RNA isolation and reverse transcription-quantitative polymerase chain reaction (RT-qPCR) assay. RNA isolation and RT-qPCR were performed as previously described (24). Total RNA from the cells was isolated using TRIzol® reagent (Invitrogen; Thermo Fisher Scientific, Inc.) and reverse transcribed to cDNA using a PrimeScript RT reagent kit purchased from Takara Bio, Inc. according to the manufacture's protocol. qPCR was performed using an SYBR Premix Ex Taq II kit. The following primers were synthesised by Takara Bio, Inc.: *APC*, forward 5'-GAGAAACCCTGTCTCGAAAAAA-3', reverse 5'-AGTGCTGTTTCTATGAGTCAAC-3'; *β-catenin*, forward 5'-AGGGTGCTATTCCACGACTA-3', reverse 5'-CACCCT TCTACTATCTCCTCCAT-3'; and *β-actin*, forward 5'-TGC TCCTCCTGAGCGCAAGTA-3' and reverse 5'-CCACAT CTGCTGGAAGGTGGA-3'. Gene expression levels were analyzed using a Rotor-Gene 3000 quantitative PCR amplifier (Corbett Life Science; Qiagen, Inc.). qPCR was conducted as follows: 10 sec at 95˚C, followed by 40 cycles of denaturation at 95˚C for 5 sec and annealing at 60˚C for 30 sec. β-actin was used as the internal control. The relative expression levels of the genes were determined by the $2^{-\Delta\Delta Cq}$ method (25).

Western blot analysis. Western blot analysis was performed as previously described. Proteins from cells were isolated using RIPA lysis buffer (Beijing Solarbio Science & Technology Co. Ltd.), and proteins from tumor tissues were dissolved in RIPA lysis buffer and isolated using sonic disruption. The concentration levels were determined using the BCA method. The proteins (40 μg) were subsequently fractionated by 10% SDS-PAGE and transferred onto polyvinylidene difluoride membranes (EMD Millipore). Immunodetection was performed by blocking the membranes in 0.1% TBS-Tween 20 containing 5% nonfat milk at room temperature for 1 h, followed by incubation with primary antibodies at 4˚C overnight. The primary antibodies used were as follows: APC (1:500), β-catenin (1:500), p-β-catenin (1:500), Wnt2 (1:2,000), E-cadherin (1:1,000), vimentin (1:1,000), Axin2 (1:2,000), GSK-3β (1:2,000), cyclin D1 (1:2,000), c-Myc (1:2,000) and β-actin (1:1,000). The following morning, the membranes were incubated for 1 h at room temperature with horseradish peroxidase conjugated goat anti-mouse (cat. no. SA00001-1) or goat anti-rabbit (cat. no. SA00001-2) secondary antibody (1:5,000; Proteintech Group, Inc.) and subsequently developed using an Amersham Enhanced Chemiluminescence Western blotting detection system (GE Healthcare Life Sciences) according to the manufacturer's protocols.

Immunofluorescence assay. The cells were plated in 24-well plates at a density of 20,000 cells/ml and allowed to adhere overnight. Following treatment with BITC (0 and 5 μM) for 24 h, the cells were washed with PBS and fixed with 4% paraformaldehyde at room temperature for 30 min. The cells were permeabilised with 0.4% Triton X-100 on ice for 5 min, followed by blocking in 3% bovine serum albumin (cat. no. H1130; Beijing Solarbio Science & Technology Co.

Ltd.) at room temperature for 1 h and incubation with primary antibodies at 4˚C overnight. The primary antibodies used were as follows: APC (1:100) and β-catenin (1:100). Following a final 4-h incubation at room temperature with RBITC conjugated goat anti-mouse (1:500; cat. no. SR131; Beijing Solarbio Science & Technology Co. Ltd.) or fluorescein conjugated goat anti-rabbit (1:500; cat. no. SA00003-2; Proteintech Group Inc.) secondary antibodies, the cells were counterstained with DAPI (Beijing Solarbio Science & Technology Co. Ltd.) at room temperature for 10 min and visualized with confocal microscopy at x1,000 magnification (in six micro-fields).

In vivo xenograft mouse model. *In vivo* xenograft mouse models were established based on previously described protocols (26,27). 4T1-Luc cells ($2x10^6$/ml) were implanted in the mammary fat pads of female BALB/c mice (8 weeks old, n=32 mice) to establish the orthotopic xenograft model. On the following day, the mice were randomly grouped into four experimental groups (8 mice/group) and treated with oral gavage of vehicle (0.2 ml/20 g; negative control), cisplatin (DDP; 2 mg/kg; positive control), 1.5 mg/kg BITC or 3 mg/kg BITC every day for 28 days.

To establish the metastatic model, the same density of 4T1-Luc cells ($2x10^6$/ml) was injected into the tail vein of female BALB/c mice (8 weeks old, n=40 mice). On the next day, the mice were randomly grouped into four experimental groups (10 mice/group). Mice from each group were treated the same as the mice form the orthotopic xenograft study every other day for 35 days.

Every 7 days, D-luciferin (0.15 g/l) was injected intraperitoneally, and the mice were analyzed using a Photon Imager for luciferase activity using the Lumina II Living Image 4.0 software (PerkinElmer, Inc.). The mice were sacrificed following the final imaging day. The tumors were collected, measured, weighed and subjected to further analysis, including H&E staining, immunohistochemistry (IHC) and western blot analyses.

H&E staining. After the tumors were fixed in 4% formaldehyde at 4˚C for 24 h, they were embedded in paraffin followed by the routine method and sliced to 5 μm thickness. The sections were dewaxed with 100% xylene for 15 min three times and hydrated using a series of graded concentrations of ethanol (100% ethanol, 1 min; 100% ethanol, 1 min; 95% ethanol, 1 min; 90% ethanol, 1 min; 80% ethanol, 1 min; 70% ethanol, 1 min; distilled water, 5 min) at room temperature. Following deparaffinization and rehydration, the sections were stained with hematoxylin at room temperature for 5 min, immersed five times in a solution of 1% HCl and 70% ethanol and subsequently rinsed with distilled water. Then the sections were stained with eosin at room temperature for 2 min. Following dehydration, the sections were treated with 100% xylene at room temperature for 2 min three times. A light microscope (AX80; Olympus Corporation) was used to examine the histopathological morphology at a magnification of x400. The images were digitized and quantified using ImageJ (National Institutes of Health).

IHC and terminal deoxynucleotidyl transferase-mediated dUTP nick end labeling (TUNEL) assay. For IHC analysis, tumors were fixed in 4% formaldehyde at 4˚C for 24 h and embedded in paraffin. The sections (5 μm) were subjected to antigen retrieval. Citrate buffer (pH 6.0) was used to retrieve antigen as a repair solution. The antigen was placed in an autoclave for 15 min. Following antigen retrieval, the sections were incubated with 3% H_2O_2 at room temperature for 10 min to block endogenous peroxidase activity and 1% bovine serum albumin (Wuhan Boster Biological Technology, Ltd.) at room temperature for 1 h to block non-specific binding. Anti-APC antibody (1:200) and anti-β-catenin antibody (1:200) were added dropwise to the sections and incubated at 4˚C overnight. According to the protocol of an IHC three-step detection kit (SP9001 and SP9002; Zhongshan Jinqiao Bio-Technology Co., Ltd.), the section was incubated with 100 μl antibodies at room temperature for 1 h. Subsequently, the sections were exposed to 3,3-diaminobenzidine (cat. no. ZLI-9017; Zhongshan Jinqiao Bio-Technology Co., Ltd.) for 5-10 min and observed under a light microscope (AX80; Olympus Corporation) at x400 magnification. At least four random, nonoverlapping representative images were captured using Image-Pro Plus software, version 6.0 (Media Cybernetics, Inc.) for the quantification of protein expression. The images corresponded to each tumor section from the eight tumors of each group.

TUNEL assays were performed according to the manufacturer's protocol (Roche Diagnostics). The 5 μm paraffin-embedded sections were fully dewaxed and hydrated, soaked in 3% H_2O_2 at room temperature for 30 min to inhibit endogenous peroxidase activity. After rinsing in PBS three times at room temperature for 5 min, the sections were treated with proteinase K (Sigma-Aldrich; Merck KGaA) at 37˚C for 15 min. After rinsing in PBS three times at room temperature for 5 min, the sections were soaked in the TdT buffer for 10 min and then incubated at 37˚C for 1 h in a moist chamber with 50 μl of the TdT buffer containing TdT (Roche Diagnostics). After further rinsing in PBS three times for 5 min, the sections were dipped in DAB at room temperature for 3-4 min and the nuclei were counterstained with hematoxylin buffer at room temperature for 10 sec. The samples were detected and analyzed using an Olympus microscope (AX80; Olympus Corporation) at x400 magnification (in six micro-fields).

Statistical analysis. All experiments were performed in triplicates. Statistical analyses were performed using Microsoft Excel software, version 2016 (Microsoft Corporation). Significant differences were analyzed using one-way ANOVA and a post-hoc Bonferroni test. $P<0.05$ was considered to indicate a statistically significant differences. The results were presented as the mean ± standard deviation of triplicate experiments performed three times.

Results

BITC inhibits the proliferation of murine mammary carcinoma cells in vitro and in vivo. MTT and clonogenicity assays were conducted to assess the antitumorigenic effects of BITC on 4T1-Luc cells *in vitro*. In response to BITC treatment, the survival of 4T1-Luc cells was significantly inhibited in a concentration-dependent manner (Fig. 1A). At concentrations of BITC >10 μM, the survival rate was <50%. As indicated in Fig. 1B, a clonogenicity assay indicated

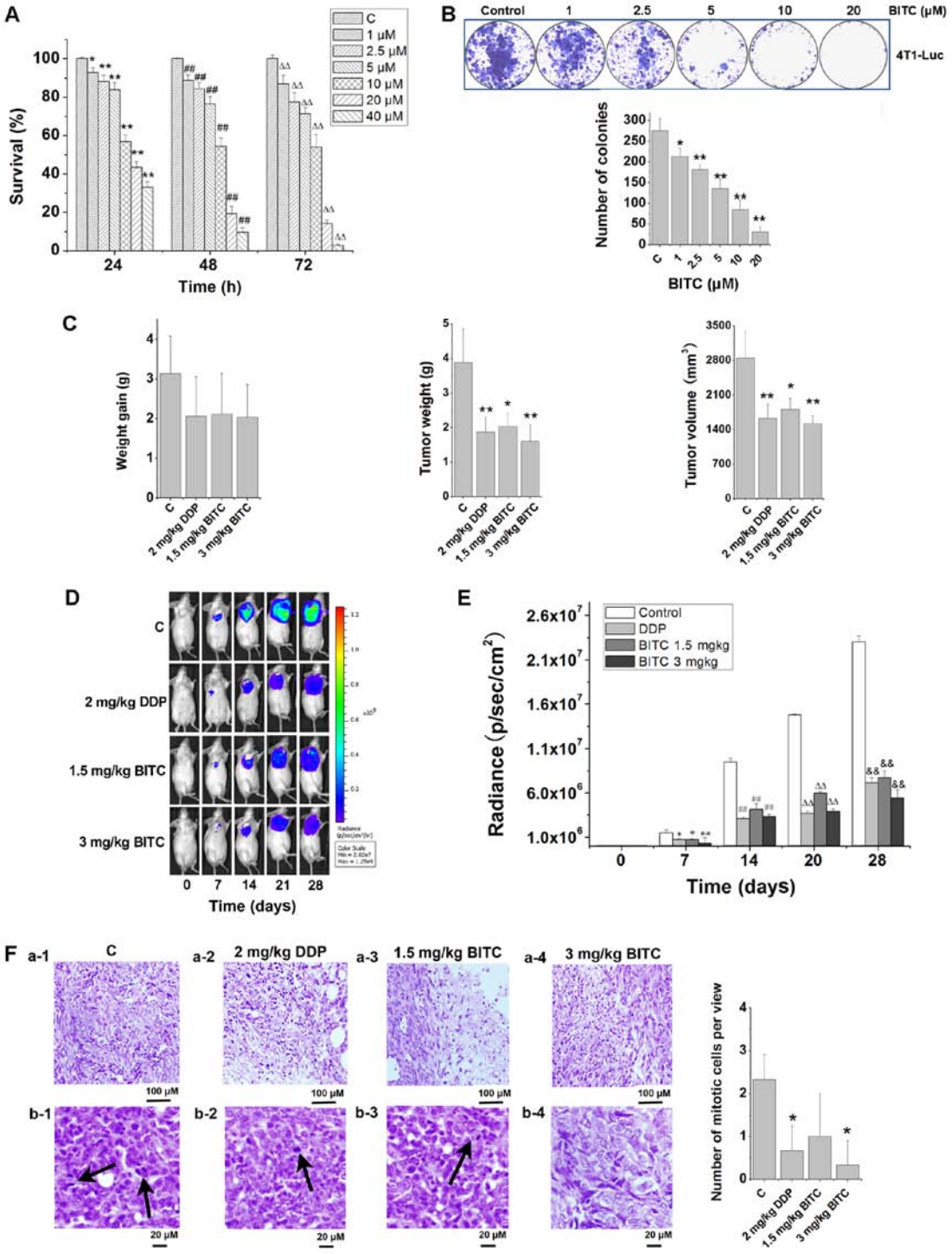

Figure 1. BITC serves an antitumorigenic role by inhibiting the proliferation and growth of 4T1-Luc cells *in vitro* and *in vivo*. (A) BITC inhibited the proliferation of 4T1-Luc cells in a concentration-dependent manner. The viability of 4T1-Luc cells treated with various concentrations of BITC for 24, 48 and 72 h was detected using an MTT assay. N=3/group. *P<0.05, **P<0.01 vs. C (24 h); $^{\#\#}$P<0.01 vs. C (48 h); $^{\Delta\Delta}$P<0.01 vs. C (72 h). (B) Clonogenicity of 4T1-Luc cells treated with various concentrations of BITC. *P<0.05, **P<0.01 vs. Control. (C) BITC inhibits the growth of xenograft tumors formed by 4T1-Luc cells *in vivo*. The antitumorigenic actions of BITC and DDP were detected by measuring (left to right): Weight gain; tumor weight; and tumor volume. N=8/group. *P<0.05, **P<0.01 vs. C. (D) Tumors were dynamically detected via bioluminescence *in vivo* imaging every 7 days (n=8 mice/group). (E) Tumor growth was monitored via bioluminescence *in vivo* imaging for 4 weeks, and the radiance (p/sec/cm^2) detected from the tumors was analyzed. *P<0.05, **P<0.01 vs. Control (7 days); $^{\#\#}$P<0.01 vs. Control (14 days); $^{\Delta\Delta}$P<0.01 vs. Control (21 days); $^{\&\&}$P<0.05 vs. Control (28 days). (F) Tumor sections were analyzed via H&E staining. a-1-4, necrosis in control, DDP, 1.5 mg/kg BITC and 3 mg/kg BITC group tissues. b-1-4, mitotic cells in control, DDP, 1.5 mg/kg BITC and 3 mg/kg BITC group tissues (x400). Arrows indicate mitotic cells. *P<0.05 vs. C. Data are presented as the mean ± standard deviation. BITC, benzyl isothiocyanate; C, control; DDP, cisplatin.

that BITC significantly suppressed the colony formation of 4T1-Luc cells. Consistent with the *in vitro* results, BITC demonstrated antitumorigenic effects *in vivo*. Following treatment with 1.5 or 3 mg/kg BITC, the growth of 4T1-Luc cell tumors in BALB/c mice of the orthotopic xenograft model was significantly inhibited, as determined by tumor

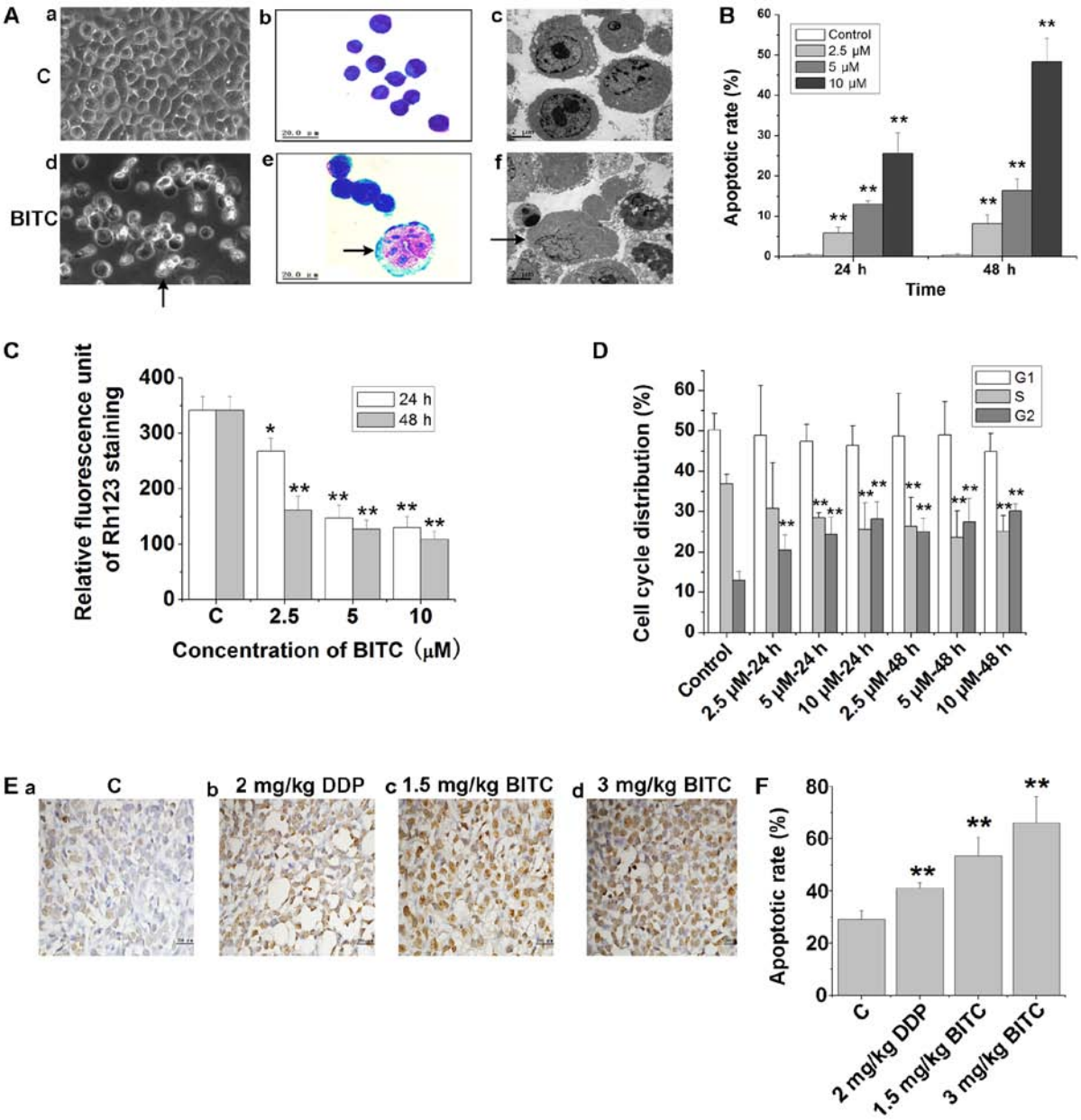

Figure 2. BITC induces the apoptosis of 4T1-Luc cells. (A) Morphological alterations of 4T1-Luc cells treated with or without BITC. (a) and (d) Morphological changes detected by phase contrast microscopy (x200). (b) Untreated and (e) BITC-treated cells were stained by Wright-Giemsa staining and recorded by light microscopy (x1,000). (c) and (f) Ultrastructural changes of 4T1-Luc cells detected by transmission electron microscopy (x5,000). Arrows indicate apoptotic cells. (B) 4T1-Luc cells were treated with various concentrations of BITC for 24 and 48 h, and apoptosis was analyzed via Annexin V/PI double staining. **P<0.01 vs. Control. (C) Mitochondrial transmembrane potential of 4T1-Luc cells treated with various concentrations of BITC for 24 and 48 h was detected via flow cytometry using Rh123 staining. *P<0.05, **P<0.01 vs. C. (D) BITC induced cell cycle arrest in 4T1-Luc cells. 4T1-Luc cells were treated as indicated and subjected to cell cycle analysis. **P<0.01 vs. Control. (E) Tumor sections were assessed via TUNEL staining to determine the number of apoptotic cells (magnification, x400). (F) Quantification of TUNEL staining in tumor sections. **P<0.01 vs. Control. BITC, benzyl isothiocyanate; C, control; DDP, cisplatin; PI, propidium iodide; Rh123, rhodamine 123.

volume and estimated tumor weight (Fig. 1C). Every 7 days, the tumors were monitored dynamically using an *in vivo* optical bioluminescence imaging system. The results further indicated that BITC treatment inhibited tumor growth in mice (Fig. 1D and E). Following animal sacrifice, the tumors were separated. H&E staining demonstrated that tumors from 3 mg/kg BITC-treated mice displayed significantly decreased numbers of mitotic cells (Fig. 1F). The necrosis phenomena in BITC-treated mice were not as clear as the control mice. Thus, we inferred that BITC may inhibit necrosis.

BITC induces 4T1-Luc cell apoptosis in vitro and in vivo. The induction of 4T1-Luc cell apoptosis following BITC treatment was demonstrated by phase-contrast microscopy and light microscopy using Right-Giemsa staining (Fig. 2A). The formation of the apoptotic bodies was apparent in BITC-treated 4T1-Luc cells using transmission electron microscopy (Fig. 2A). Flow cytometry using Annexin V-FITC and PI staining indicated that BITC treatment induced apoptosis in 4T1-Luc cells, with the apoptotic rate significantly increased following treatment with 2.5, 5 and 10 μM BITC (Fig. 2B). Alterations in the MTP are also apoptotic indicators; the use of

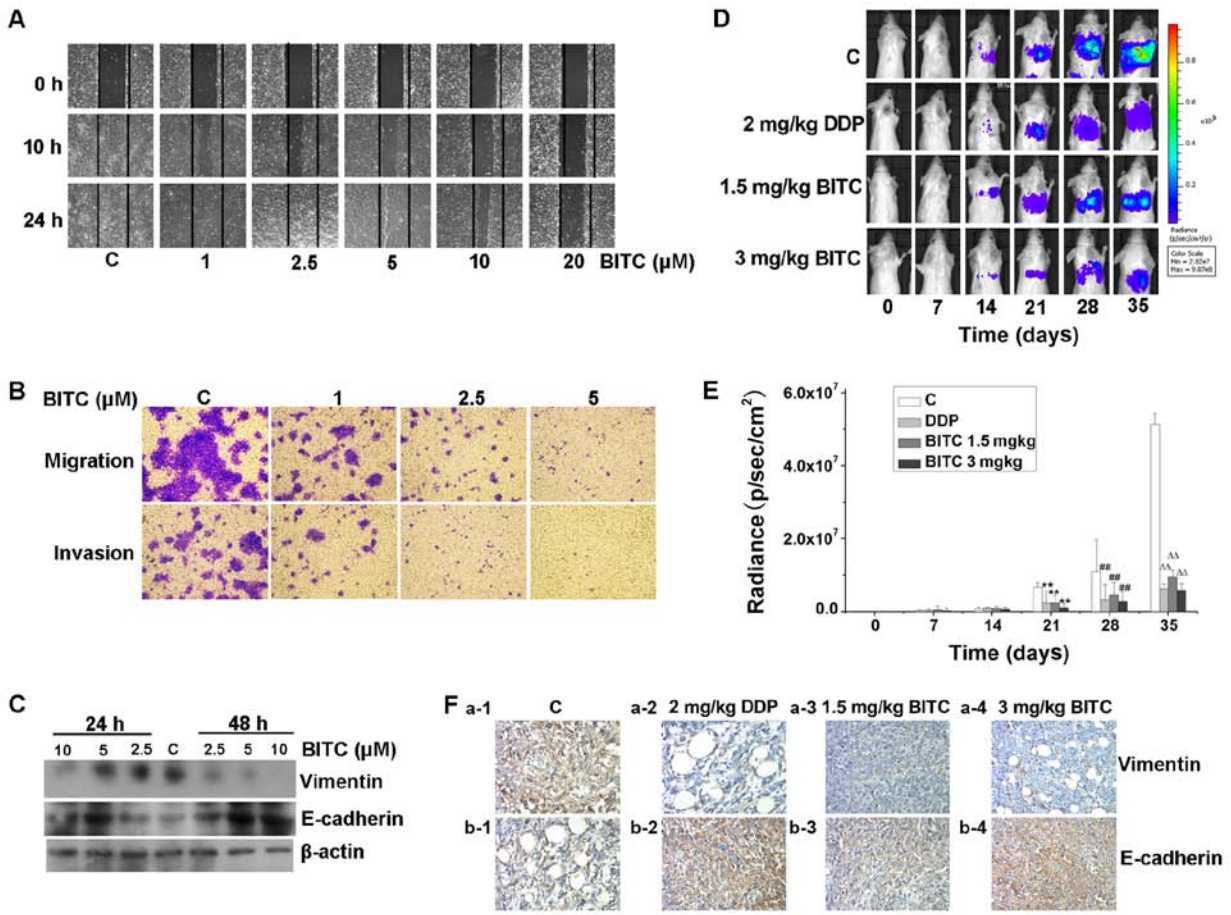

Figure 3. BITC inhibits the migration, invasion and metastasis of 4T1-Luc cells. (A) BITC inhibited the migration of 4T1-Luc cells. 4T1-Luc cells were treated with BITC as indicated and subjected to a wound healing assay (x100). (B) BITC inhibited the migration and invasion of murine mammary carcinoma cells. 4T1-Luc cells were cultured in Transwell chambers coated with or without Matrigel for 24 h, in the presence of the indicated concentrations of BITC (x40). (C) BITC inhibited cellular migration by regulating the expression levels of vimentin and E-cadherin. 4T1-Luc cells were treated with various concentrations of BITC as indicated for 24 and 48 h. Total protein lysates were immunoblotted for E-cadherin and vimentin expression. β-actin was used as the internal control. (D) Inhibitory effects of BITC on the metastasis of murine mammary carcinoma in mice was monitored using an optical in vivo bioluminescence imaging system every 7 days (n=8 mice/group). (E) Quantification of radiance recorded from the tumors were analyzed. **P<0.01 vs. C (21 days); $^{\#\#}$P<0.01 vs. C (28 days); $^{\Delta\Delta}$P<0.01 vs. C (35 days). (F) Tumor sections were assessed via immunohistochemistry to determine the expression of E-cadherin and vimentin. The expression of E-cadherin was upregulated, whereas that of vimentin was downregulated in BITC-treated mice compared with those in the control group (magnifcation, x400). BITC, benzyl isothiocyanate; C, control; DDP, cisplatin.

Rh123 reveals the changes to the MTP. The results indicated that the mitochondrial transmembrane potential was significantly depolarized in BITC-treated 4T1-Luc cells compared with untreated cells, suggesting that BITC treatment induced the apoptosis of 4T1-Luc cells (Fig. 2C). BITC treatment also altered the cell cycle distribution of 4T1-Luc cells (Fig. 2D). BITC treatment led to cell cycle arrest and the accumulation of 4T1-Luc cells at the G2/M phase compared with the cell cycle distribution of control-treated 4T1-Luc cells. *In vivo*, TUNEL staining of tumor sections indicated that the number of TUNEL-positive apoptotic cells in BITC-treated mice was significantly increased compared with in non-treated mice (Fig. 2E and F).

BITC suppresses the migration, invasion and metastasis of 4T1-Luc cells by activating E-cadherin and inhibiting the expression of vimentin. BITC treatment markedly inhibited the mobility of 4T1-Luc cells in a concentration-dependent manner (Fig. 3A). The effects of BITC were assessed on the migration and invasion of cells. Transwell chambers coated with collagen or Matrigel were used and as presented in Fig. 3B, the migratory and invasive abilities of 4T1-Luc cells were notably inhibited following BITC treatment. Consistent with the *in vitro* results, the *in vivo* studies further revealed that BITC inhibited the metastasis of murine mammary carcinoma, as demonstrated using an *in vivo* optical bioluminescence imaging system (Fig. 3D and E). The expression levels of the metastasis inhibitor E-cadherin were increased, whereas the expression levels of the metastasis promoter vimentin (28) were decreased in BITC-treated cells and tissues (Fig. 3C and F). These results suggested that the metastasis-inhibitory effects of BITC on murine mammary carcinoma were mediated by upregulating E-cadherin and downregulating vimentin expression levels.

BITC induces antitumorigenic effects by regulating the Wnt/β-catenin pathway. The Wnt signaling pathway serves an important role in carcinogenesis (17). The expression levels of its signaling transducers were evaluated in BITC-treated cells and tumor-bearing mice. Western blotting indicated that the

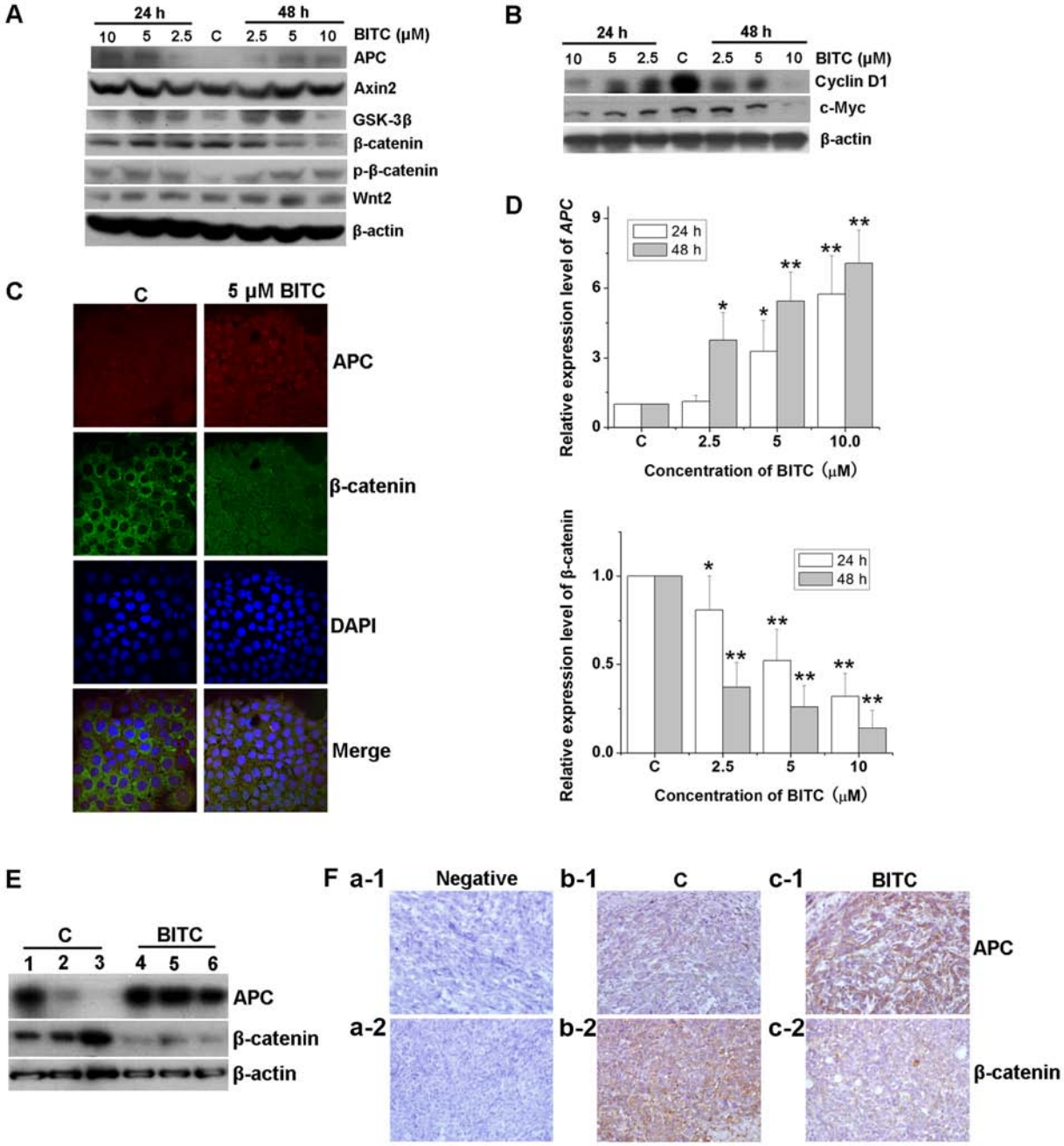

Figure 4. BITC regulates the Wnt/β-catenin pathway and the APC/β-catenin complex. 4T1-Luc cells were treated with various concentrations of BITC as indicated for 24 and 48 h. Total protein lysates were immunoblotted for (A) APC, Axin2, GSK-3β, β-catenin, p-β-catenin and Wnt2, and (B) cyclin D1 and c-Myc protein expression. β-actin was used as the internal control. (C) Immunofluorescence assay was performed to evaluate the expression and subcellular location of APC and β-catenin protein (magnification, x1,000). (D) 4T1-Luc cells were treated with various concentrations of BITC as indicated for 24 and 48 h, and total RNA was isolated and reverse transcribed. The mRNA expression levels of *APC* and *β-catenin* were detected via reverse transcription-quantitative PCR analysis. *P<0.05, **P<0.01 vs. C. (E) Protein lysates isolated from the tumors of control or BITC-treated mice were subjected to western blot analysis for APC and β-catenin. 1-6 indicated different mice. (F) Tumors from control and BITC-treated mice were subjected to immunohistochemical analysis using APC and β-catenin antibodies (magnification, x400). APC, adenomatous polyposis coli; BITC, benzyl isothiocyanate; C, control; DAPI, 4',6-diamidino-2-phenylindole; GSK-3β, glycogen synthase kinase-3β.

expression levels of APC and GSK-3β were notably increased in 4T1-Luc cells following BITC treatment compared with those in control cells (Fig. 4A), whereas the expression of the tumor promoters β-catenin and Wnt2 was inhibited in response to BITC treatment. The expression levels of Axin2 were markedly unaffected. Additionally, the phosphorylation levels of β-catenin were markedly upregulated, whereas those of the downstream factors of β-catenin, such as cyclin D1 and c-Myc were downregulated (Fig. 4B). Immunofluorescence staining demonstrated that the expression levels of APC were markedly increased, whereas those of β-catenin were decreased (Fig. 4C). In addition, β-catenin protein appeared to be partially transferred from the cytoplasmic to the nuclear region (Fig. 4C). The mRNA expression levels of *APC* and *β-catenin* were detected via RT-qPCR analysis. The transcriptional levels of *APC* and *β-catenin* in BITC-treated 4T1-Luc

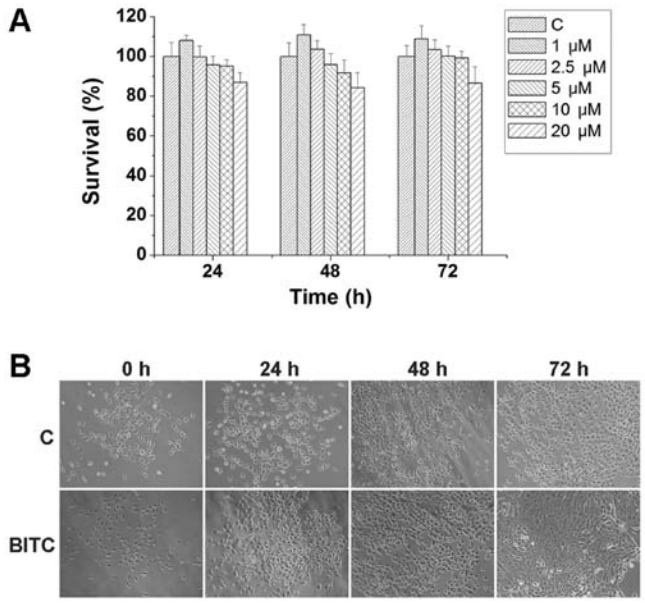

Figure 5. BITC does not induce toxicity or side effects in MCF-10A cells. (A) Effects of BITC on MCF-10A cells at 24, 48 and 72 h were detected using an MTT assay. Data are presented as the mean ± standard deviation (n=3). (B) Phase contrast microscopy was used to detect the morphological changes of MCF-10A cells treated with or without BITC for 0, 24, 48 and 72 h (x100). BITC, benzyl isothiocyanate; C, control.

cells were significantly increased and decreased, respectively (Fig. 4D), in accordance with the aforementioned alterations observed at the translational level. Western blotting indicated that the expression levels of APC and β-catenin were notably increased and decreased, respectively in tumors from BITC-treated mice compared with controls (Fig. 4E). IHC staining further indicated that in BITC-treated mice, APC expression was upregulated, whereas that of β-catenin was downregulated (Fig. 4F), suggesting that BITC may serve antitumorigenic roles in murine mammary carcinoma cells by regulating the Wnt/β-catenin pathway and the APC-GSK-3β degradation complex.

BITC does not induce toxicity or side effects in the normal mammary epithelial cell line MCF-10A. To investigate whether BITC treatment affects normal mammary epithelial cells, MCF-10A cells were treated with various concentrations of BITC for 24, 48 and 72 h. As indicated in Fig. 5A, BITC treatment did not induce significant inhibitory effects on the viability of MCF-10A cells. The morphological differences detected by phase contrast microscopy indicated that MCF-10A cells treated with BITC exhibited no morphological alterations compared with control cells (Fig. 5B).

Discussion

BITC is a compound found in cruciferous vegetables that has been reported to possess antitumor properties (7-15). Administration of BITC suppresses the incidence, growth and metastasis of cancer cells (8,9). Warin *et al* (7) reported that BITC prevented mammary carcinogenesis in MMTV-neu mice. Kim *et al* (9) demonstrated that oral BITC treatment induced a significant reduction in the growth of solid tumors. In the present study, it was demonstrated that the growth of 4T1-Luc xenografts was significantly inhibited following BITC treatment. The weight and the volume of the tumors in BITC-treated and DDP-treated BALB/c mice were significantly decreased compared with those in untreated mice. As 4T1 cells were transfected with luciferase, tumor growth could be observed conveniently and dynamically using an optical *in vivo* bioluminescence imaging system. The results suggested that tumor growth was significantly inhibited. These *in vivo* experiments demonstrated that BITC induced antitumor effects in murine mammary carcinoma.

BITC exhibited diverse mechanisms of action in various types of cancer. Previous studies revealed that BITC inhibited neoplasm formation by activating or inhibiting various signaling pathways and/or processes, including the impairment of ROS production, disruption of mitochondrial function, inhibition of the PI3K, regulation of the MAPK signaling pathway and activation of the p53 pathway (11,12,14,15,29,30). Kim *et al* (9) demonstrated that BITC induced murine mammary cell apoptosis, reduced the number of pulmonary tumor nodules and decreased the total pulmonary metastatic volume. Additionally, BITC induced alterations in the expression levels of indicators of apoptosis and metastasis (9); however, the authors did not determine the underlying mechanism of actions of BITC in 4T1 cells. In the present study, it was revealed that the expression levels of several factors involved in the Wnt signaling pathway were altered in murine mammary carcinoma cells in response to BITC treatment. The expression levels of the proteins APC and GSK-3β were increased, whereas the expression levels of β-catenin were decreased, indicating that BITC activated the degradation complex and regulated the Wnt signaling pathway in order to perform its tumor-preventive and tumor-inhibitory roles.

The dysregulation of the Wnt signaling pathway is a hallmark of various types of cancer with an aggressive phenotype (31). The Wnt signaling transduction pathway has been reported to serve a vital role in homeostasis via multiple modes of action (32). The β-catenin-dependent canonical pathway has been extensively studied compared with other signaling pathways. APC, GSK-3β and β-catenin form a destruction complex, which regulates the activity of β-catenin. The destruction complex phosphorylates β-catenin, inducing a reduction in its levels in the cytoplasmic and nuclear regions, and resulting in the downregulation of its downstream targets, including cyclin D1 and c-Myc (17,19,32). The results of the present study indicated that BITC promoted the phosphorylation of β-catenin and decreased its levels. In response to BITC, β-catenin might target the genes cyclin D1 and c-Myc, and downregulated their expression, though further investigation is required. The present findings were consistent with results reported in previous studies regarding the ability of BITC treatment to reduce the expression levels of FOXH1 (22), which in turn significantly increased the expression levels of β-catenin, cyclin D1 and c-Myc proteins in MCF7 and MDA-MB-231 cells (22). By regulating the induction of the Wnt/β-catenin pathway via FOXH1, BITC exposure suppressed cell growth and invasion in human breast cancer cells (22).

Curcumin is a naturally occurring phenolic compound, which regulates the Wnt/β-catenin pathway via metastasis associated protein 1 and suppresses proliferation and invasion

in non-small cell lung cancer (33). Caudatin is a C-21 steroidal glycoside isolated from Chinese herbs, which can induce apoptosis in gastric cancer cells by modulating the Wnt/β-catenin signaling (34). In the present study, it was reported that BITC inhibited proliferation, induced cell cycle arrest and apoptosis, and disrupted the MTP in murine mammary carcinoma cells by regulating the Wnt/β-catenin signaling pathway. It was revealed that BITC inhibited the proliferation of 4T1-Luc cells in a concentration-dependent manner, and that it induced cell cycle arrest in 4T1-Luc cells at the G2/M phase. In addition, it was further demonstrated that BITC induced apoptosis in murine mammary carcinoma cells *in vitro*. To validate these findings, the induction of apoptosis in tumor samples was investigated. TUNEL staining demonstrated that the apoptotic rate was significantly increased in BITC-treated tumor samples. The expression levels of β-catenin in tumor samples treated with BITC were significantly decreased, whereas those of APC were increased. Collectively, the results suggested that BITC inhibited tumor growth and induced apoptosis in murine mammary carcinoma *in vitro* and *in vivo,* and that the Wnt/β-catenin pathway was involved in the antitumor effects of BITC. As previously reported (7-10), BITC exerts antitumor properties in the absence of notable side effects or toxicity. Consistent with this, it was demonstrated that BITC did not significantly affect the survival or morphology of normal mammary epithelial cells *in vitro*.

A previous study reported that homeodomain-interacting protein kinase-2 knockdown induced Wnt signaling activation and β-catenin nuclear localisation, promoted cell invasion and decreased E-cadherin expression (35). Paired-related homeobox 1 is an EMT inducer that has been demonstrated to promote EMT in gastric cancer cells via the activation of the Wnt/β-catenin signaling pathway, and the regulation of the EMT molecular markers E-cadherin and vimentin (36). These studies indicated that the Wnt signaling pathway promoted metastasis. In the present study, wound healing, Matrigel-invasion and migration assays were performed, and it was observed that BITC inhibited the migration of murine mammary carcinoma cells. This was further supported by the *in vivo* results. Western blot analyses indicated that the expression levels of E-cadherin were increased, and those of vimentin were decreased following BITC treatment. Thus, the present findings suggested that BITC may inhibit the metastasis of murine mammary carcinoma cells by regulating the Wnt/β-catenin signaling pathway, and by regulating the expression levels of E-cadherin and vimentin.

In conclusion, the present study demonstrated that BITC induced antitumorigenic effects, inhibiting proliferation, inducing cell cycle arrest, inhibiting metastasis and inducing the apoptosis of murine mammary carcinoma cells, but did not induce toxicity or side effects in normal mammary epithelial cells. In addition, the data indicated that the Wnt/β-catenin signaling pathway was activated in response to BITC treatment, providing insight into the molecular mechanisms underlying the effects of BITC on murine mammary carcinoma 4T1-Luc cells *in vitro* and *in vivo*. Despite the current data on the antitumor actions of BITC, further studies involving knockdown or overexpression models of the Wnt/β-catenin signaling pathway are required to demonstrate the exact roles of the Wnt/β-catenin pathway in the induction of apoptosis or the inhibition of metastasis mediated by BITC. As BITC was reported to phosphorylate β-catenin, decrease β-catenin levels, and downregulate Wnt2, cyclin D1 and c-Myc, it was suggested that BITC exerted its antitumor properties by regulating the Wnt/β-catenin signaling pathway; however, previous studies indicated that the expression levels of cyclin D1, c-myc and β-catenin were regulated by specificity protein (Sp) transcription factors during antitumor processes (37). Therefore, whether BITC regulates Sp to mediate its antitumorigenic effects also requires further investigation.

Acknowledgements

The authors would like to thank Dr Dimiter Avtanski of Hofstra Northwell School of Medicine (New York, USA) for his meticulous language editing and revision of the manuscript.

Funding

The present work was supported by the Fundamental Research Funds of the Central Universities from the Lanzhou University (grant no. lzujbky-2017-142), the Science and Technology Planning Project from Chengguan District, Lanzhou, Gansu Province, China (grant no. 2016-7-11) and the Natural Science Fund of Gansu (grant no. 17JR5RA192). These funds were used to design the study and collect the data.

Availability of data and materials

All data generated or analyzed during this study are included in this published article.

Authors' contributions

HLW made substantial contributions towards the conception and design of the study, revised the paper critically and provided approval for the final version to be submitted. BX planned the study, designed and performed the experiments, acquired the data, analyzed the results and drafted the manuscript. LZ, LLG, HL, SYF, WJF, LL, JC, BW and LLF participated in performing the experiments, interpreting the data, and drafting and revising the manuscript.

Ethics approval and consent to participate

All the animal procedures were ethically approved by the Laboratory Animal Science and Technology Management Committee of the Lanzhou University School of Basic Medical Sciences, and conducted in accordance with the Guide for Care and Use of Laboratory Animals (8th Edition).

Patient consent for publication

Not applicable.

Competing interests

The authors declare that they have no competing interests.

References

1. Avtanski DB, Nagalingam A, Bonner MY, Arbiser JL, Saxena NK and Sharma D: Honokiol inhibits epithelial-mesenchymal transition in breast cancer cells by targeting signal transducer and activator of transcription 3/Zeb1/E-cadherin axis. Mol Oncol 8: 565-580, 2014.
2. Nagalingam A, Arbiser JL, Bonner MY, Saxena NK and Sharma D: Honokiol activates AMP-activated protein kinase in breast cancer cells via an LKB1-dependent pathway and inhibits breast carcinogenesis. Breast Cancer Res 14: R35, 2012.
3. Chen H and Liu RH: Potential mechanisms of action of dietary phytochemicals for cancer prevention by targeting cellular signaling transduction pathways. J Aqric Food Chem 66: 3260-3276, 2018.
4. Gründemann C and Huber R: Chemoprevention with isothiocyanates-from bench to bedside. Cancer Lett 414: 26-33, 2018.
5. Soundararajan P and Kim JS: Anti-carcinogenic glucosinolates in cruciferous vegetables and their antagonistic effects on prevention of cancers. Molecules 23: pii: E2983, 2018.
6. Jutooru I, Guthrie AS, Chadalapaka G, Pathi S, Kim K, Burghardt R, Jin UH and Safe S: Mechanism of action of phenethylisothiocyanate and other reactive oxygen species-inducing anticancer agents. Mol Cell Biol 34: 2382-2395, 2014.
7. Warin R, Chambers WH, Potter DM and Singh SV: Prevention of mammary carcinogenesis in MMTV-neu mice by cruciferous vegetable constituent benzyl isothiocyanate. Cancer Res 69: 9473-9480, 2009.
8. Ni WY, Hsiao YP, Hsu SC, Hsueh SC, Chang CH, Ji BC, Yang JS, Lu HF and Chuang JG: Oral administration of benzyl-isothiocyanate inhibits in vivo growth of subcutaneous xenograft tumors of human malignant melanoma A375.S2 cells. In Vivo 27: 623-626, 2013.
9. Kim KJ, Hong JE, Eom SJ, Lee JY and Park JH: Oral administration of benzyl-isothiocyanate inhibits solid tumor growth and lung metastasis of 4T1 murine mammary carcinoma cells in BALB/c mice. Breast Cancer Res Treat 130: 61-71, 2011.
10. Kim M, Cho HJ, Kwon GT, Kang YH, Kwon SH, Her S, Park T, Kim Y, Kee Y and Park JH: Benzyl isothiocyanate suppresses high-fat diet-stimulated mammary tumor progression via the alteration of tumor microenvironments in obesity-resistant BALB/c mice. Mol Carcinog 54: 72-82, 2015.
11. Liu X, Takano C, Shimizu T, Yokobe S, Abe-Kanoh N, Zhu B, Nakamura T, Munemasa S, Murata Y and Nakamura Y: Inhibition of phosphatidylinositide 3-kinase ameliorates antiproliferation by benzyl isothiocyanate in human colon cancer cells. Biochem Biophys Res Commun 491: 209-216, 2017.
12. Xie B, Nagalingam A, Kuppusamy P, Muniraj N, Langford P, Győrffy B, Saxena NK and Sharma D: Benzyl Isothiocyanate potentiates p53 signaling and antitumor effects against breast cancer through activation of p53-LKB1 and p73-LKB1 axes. Sci Rep 7: 40070, 2017.
13. Zhu M, Li W, Dong X, Chen Y, Lu Y, Lin B, Guo J and Li M: Benzyl-isothiocyanate induces apoptosis and inhibits migration and invasion of hepatocellular carcinoma cells in vitro. J Cancer 8: 240-248, 2017.
14. Kasiappan R, Jutooru I, Karki K, Hedrick E and Safe S: Benzyl isothiocyanate (BITC) induces reactive oxygen species-dependent repression of STAT3 protein by down-regulation of specificity proteins in pancreatic cancer. J Biol Chem 291: 27122-27133, 2016.
15. Lai KC, Hsiao YT, Yang JL, Ma YS, Huang YP, Chiang TA and Chung JG: Benzyl isothiocyanate and phenethyl isothiocyanate inhibit murine melanoma B16F10 cell migration and invasion *in vitro*. Int J Oncol 51: 832-840, 2017.
16. Ma YS, Hsiao YT, Lin JJ, Liao CL, Lin CC and Chung JG: Phenethyl iosthiocyanate (PEITC) and Benzyl isothiocyanate (BITC) inhibit human melanoma A375.S2 cell migration and invasion by affecting MAPK signaling pathway in vitro. Anticancer Res 37: 6223-6234, 2017.
17. Duchartre Y, Kim YM and Kahn M: The Wnt signaling pathway in cancer. Crit Rev Oncol Hematol 99: 141-149, 2016.
18. Lee MA, Kim WK, Park HJ, Kang SS and Lee SK: Anti-proliferative activity of hydnocarpin, a natural lignan, is associated with the suppression of Wnt/β-catenin signaling pathway in colon cancer cells. Bioorg Med Chem Lett 23: 5511-5514, 2013.
19. Schmitz Y, Rateitschak K and Wolkenhauer O: Analysing the impact of nucleo-cytoplasmic shuttling of β-catenin and its antagonists APC, Axin and GSK3 on Wnt/β-catenin signaling. Cell Signal 25: 2210-2221, 2013.
20. Bilir B, Kucuk O and Moreno CS: Wnt signaling blockage inhibits cell proliferation and migration, and induces apoptosis in triple-negative breast cancer cells. J Transl Med 11: 280, 2013.
21. Liu QQ, Chen K, Ye Q, Jiang XH and Sun YW: Oridonin inhibits pancreatic cancer cell migration and epithelial-mesenchymal transition by suppressing Wnt/β-catenin signaling pathway. Cancer Cell Int 16: 57, 2016.
22. Liu Y, Zhang L, Meng Y and Huang L: Benzyl isothiocyanate inhibits breast cancer cell tumorigenesis via repression of the FoxH1-Mediated Wnt/β-catenin pathway. Int J Clin Med 8: 17601-17611, 2015.
23. National Research Council (US) Committee for the Update of the Guide for the Care and Use of Laboratory Animals. Guide for the Care and Use of Laboratory Animals, 8th edition. National Academies Press (US), 2011.
24. Chen J, Cheng J, Yi J, Xie B, Lin L, Liu Z, Zhao H, Wang B, Ai Z, Yang Y and Wei H: Differential expression and response to arsenic stress of MRPs and ASAN1 determine sensitivity of classical multidrug-resistant leukemia cells to arsenic trioxide. Leuk Res 50: 116-122, 2016.
25. Livak KJ and Schmittgen TD: Analysis of relative gene expression data using real-time quantitative PCR and the 2(-Delta Delta C(T)) method. Methods 25: 402-408, 2001.
26. Kocatürk B and Versteeg HH: Orthotopic injection of breast cancer cells into the mammary fat pad of mice to study tumor growth. J Vis Exp, Feb 8, 2015. doi: 10.3791/51967.
27. Rios Garcia M, Steinbauer B, Srivastava K, Singhal M, Mattijssen F, Maida A, Christian S, Hess-Stumpp H, Augustin HG, Müller-Decker K, *et al*: Acetyl-CoA Carboxylase 1-dependent protein acetylation controls breast cancer metastasis and recurrence. Cell Metab 26: 842-855.e5, 2017.
28. Zhou J, Tao D, Xu Q, Gao Z and Tang D: Expression of E-cadherin and vimentin in oral squamous cell carcinoma. Int J Clin Exp Pathol 8: 3150-3154, 2015.
29. Huang SH, Wu LW, Huang AC, Yu CC, Lien JC, Huang YP, Yang JS, Yang JH, Hsiao YP, Wood WG, *et al*: Benzyl isothiocyanate (BITC) induces G2/M phase arrest and apoptosis in human melanoma A375.S2 cells through reactive oxygen species (ROS) and both mitochondria-dependent and death receptor-mediated multiple signaling pathways. J Agric Food Chem 60: 665-675, 2012.
30. Hedrick E, Cheng Y, Jin UH, Kim K and Safe S: Specificity protein (Sp) transcription factors Sp1, Sp3 and Sp4 are non-oncogene addiction genes in cancer cells. Oncotarget 7: 22245-22256, 2016.
31. Valencia A, Román-Gómez J, Cervera J, Such E, Barragán E, Bolufer P, Moscardó F, Sanz GF and Sanz MA: Wnt signaling pathway is epigenetically regulated by methylation of Wnt antagonists in acute myeloid leukemia. Leukemia 23: 1658-1666, 2009.
32. Mahmood S, Bhatti A, Syed NA and John P: The microRNA regulatory network: A far-reaching approach to the regulate the Wnt signaling pathway in number of diseases. J Recept Signal Transduct Res 36: 310-318, 2016.
33. Lu Y, Wei C and Xi Z: Curcumin suppresses proliferation and invasion in non-small cell lung cancer by modulation of MTA1-mediated Wnt/β-catenin pathway. In Vitro Cell Dev Biol Anim 50: 840-850, 2014.
34. Li X, Zhang X, Liu X, Tan Z, Yang C, Ding X, Hu X, Zhou J, Xiang S, Zhou C and Zhang J: Caudatin induces cell apoptosis in gastric cancer cells through modulation of Wnt/β-catenin signaling. Oncol Rep 30: 677-684, 2013.
35. Tan M, Gong H, Zeng Y, Tao L, Wang J, Jiang J, Xu D, Bao E, Qiu J and Liu Z: Downregulation of homeodomain-interacting protein kinase-2 contributes to bladder cancer metastasis by regulating Wnt signaling. J Cell Biochem 115: 1762-1767, 2014.
36. Guo J, Fu Z, Wei J, Lu W, Feng J and Zhang S: PRRX1 promotes epithelial-mesenchymal transition through the Wnt/β-catenin pathway in gastric cancer. Med Oncol 32: 393, 2015.
37. Pathi S, Jutooru I, Chadalapaka G, Nair V, Lee SO and Safe S: Aspirin inhibits colon cancer cell and tumor growth and downregulates specificity protein (Sp) transcription factors. PLoS One 7: e48208, 2012.